Macromolecules **1992**, *25*, 475–478

Viscoelastic Properties of Polyelectrolyte Solutions. 2. Steady-State Compliance

Masayoshi Yamaguchi,* Michio Wakutsu, Yoshiaki Takahashi, and Ichiro Noda

Department of Applied Chemistry, Nagoya University, Furo-cho, Chikusa-ku, Nagoya 464-01, Japan

Received May 14, 1991; Revised Manuscript Received September 17, 1991

ABSTRACT: Steady-state compliance J_e of polyelectrolyte solutions was measured in the presence and absence of added salt. In dilute regions, J_e depends on molecular weight M, polymer concentration C, and concentration of added salt C_s. The M and C dependences are much stronger than that of nonionic polymers as given by $J_e \propto M^{-2}C^{-3}C_s$. In entangled regions, on the other hand, J_e depends on C only in the same manner as for that of nonionic polymer solutions, but the concentration dependence is weaker than that of nonionic polymers as given by $J_e \propto C^{-1.3}$. Moreover, the polymer concentration dependence of the weight-average relaxation time τ_w defined as the product of zero-shear viscosity η^0 and J_e is found to increase with increasing C_s in semidilute regions for η^0 and entangled regions for J_e. These features of J_e and τ_w in entangled regions can be explained by the same model as for zero-shear viscosity in Part 1.

Introduction

Viscoelastic properties of polymer solutions are studied in terms of zero-shear viscosity η^0 and steady-state compliance J_e representing the energy dissipation and storage, respectively. In Part 1, we measured η^0 of polyelectrolyte solutions in the absence and presence of added salt and reported that the polymer concentration dependence of η^0 increases with an increase in the concentration of added salt and it almost agrees with that for nonionic polymers in good solvents at high concentrations of added salt.

As reported in a previous paper,[2] J_e of nonionic polymer solutions is understood by classifying the solutions as two regions, i.e., dilute (not entangled) and entangled regions. In dilute regions, a polymer chain is isolated so that J_e is approximately proportional to the molecular weight M and the inverse of polymer concentration C.

$$J_e \propto MC^{-1} \tag{1}$$

$$J_{eR} \doteqdot \text{constant} \tag{2}$$

Here, we defined the reduced steady-state compliance J_{eR} as

$$J_{eR} \equiv (J_eCRT/M)[\eta^0/(\eta^0 - \eta_s)]^2 \tag{3}$$

where η_s is the solvent viscosity.

In entangled regions,[2] polymer chains form approximately a uniform network, regardless of solvent power, so that J_e is independent of the molecular weight, and it is proportional to the inverse square of C

$$J_e \propto M^0C^{-2} \tag{4}$$

and, hence

$$J_{eR} \propto (CM)^{-1} \tag{5}$$

Thus, J_{eR} is expressed as a universal function of CM. Moreover, it was reported that the crossover concentration from dilute to entangled regions at constant molecular weight is about 5 times higher than that for η^0.[2]

The elastic properties are expected to be affected very much by electrostatic interactions. Although there are a few studies on the elastic properties of polyelectrolyte solutions,[3–6] the sample had relatively broad molecular weight distributions and/or the ranges of polymer concentration were limited. In the present work, therefore, we measured J_e of polyelectrolyte solutions with relatively narrow molecular weight distributions at finite concentrations in the absence and presence of added salt to study the effects of electrostatic interactions to J_e in comparison with the results of nonionic polymer solutions. The weight-average relaxation time τ_w ($=\eta^0J_e$) is also discussed.

Experimental Section

Polyelectrolyte samples used were the same three poly(*N*-methyl-2-vinylpyridinium chloride)s (PMVP-Cl) with narrow molecular weight distributions as used for viscosity studies reported in Part 1.[1] The molecular characteristics of samples were shown in Table I in Part 1.[1] J_e was evaluated from the data in oscillatory flow reported previously,[1] except two J_e data obtained by measuring flow birefringence for comparison. The details of flow birefringence measurements were reported previously.[4]

Results

An example of the dependences of storage and loss moduli G' and G'' on frequency ω is shown in Figure 1. As the dependences of G' and G'' in the low-frequency regions are proportional to the second and first power of ω, respectively, J_e is evaluated from the following equations in the terminal region.

$$\eta^0 = \lim_{\omega \to 0} G''/\omega$$

$$A_g = \lim_{\omega \to 0} G'/\omega^2$$

$$J_e = A_g/(\eta^0)^2$$

As reported previously,[8] the form anisotropy of flow birefringence disappears in semidilute solutions for thermodynamic properties so that we evaluated J_e in 0.01 M

0024-9297/92/2225-0475$03.00/0

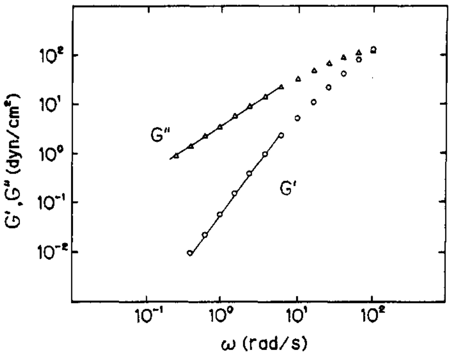

Figure 1. Example of the dependence of G' and G'' on ω. The sample is MVPK-13, C = 0.01 g/cm^3 and C_s = 0.01 M.

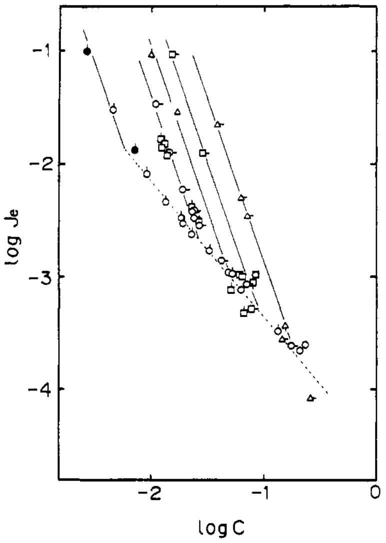

Figure 2. Polymer concentration dependence of J_e at various concentrations of added salt. The triangles, squares, and circles denote the data for MVPK-11, MVPK-12, and MVPK-13, respectively. Pips indicate the different concentrations of added salt: upward, 0.01 M; rightward, 0.1 M; downward, 0.5 M. Symbols without pips denote the data in the absence of added salt. The closed circles denote the data from the flow birefringence measurements. The solid and broken lines are drawn to smoothly connect the data in dilute and entangled regions, respectively.

NaCl aqueous solution at two polymer concentrations from the data of flow birefringence by using the relationships[9,10]

$$\eta = \Delta n \sin(2\chi)/2C'\dot{\gamma} + \eta_s$$

$$J_s = \Delta N \cos(2\chi)/2C'\eta^2\dot{\gamma}^2$$

$$J_e = \lim_{\dot{\gamma}\to 0} J_s$$

where Δn is the birefringence, χ is the extinction angle, $\dot{\gamma}$ is the shear rate, η is the viscosity of solution, and C' is the stress-optical coefficient. For PMVP-Cl in NaCl solutions, C' is 1.9×10^{-9} cm^2/dyn, which was determined by dividing $\Delta n \sin(2\chi)/2\dot{\gamma}$ by $\eta - \eta_s$ measured by a capillary viscometer of the Maron–Krieger–Sisko type.

Figure 2 shows double-logarithmic plots of J_e vs C for PMVP-Cl in 0.5, 0.1, and 0.01 M NaCl solutions and salt-free solutions. As shown in the figure, the data from the mechanical and flow birefringence measurements are in good agreement with each other. At low polymer concentrations, J_e is larger at higher concentration of added salt if the molecular weight is the same, and it decreases with an increase of the molecular weight at the same polymer and added salt concentrations. The same tendency was reported for the concentration dependence of added salt in poly(sodium acrylate) solutions.[4] At high polymer concentrations, on the other hand, J_e appears to depend on polymer concentrations only, regardless of concentrations of added salt and molecular weight, in the same manner as that of nonionic polymer solutions. If we assume that the regions where J_e depends on molecular weight are dilute ones in the same manner as that of nonionic polymer solutions, the dependences of J_e on molecular weight and the polymer concentration in dilute regions are very much different from that of nonionic polymer solutions; the molecular weight dependence is contrary to that of nonionic polymers, and the concentration dependence is much stronger.

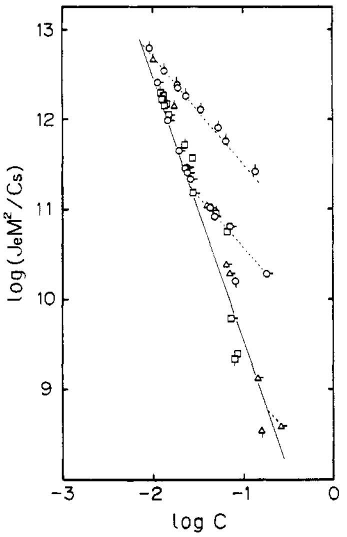

Figure 3. Double-logarithmic plots of J_eM^2/C_s vs C. Symbols are the same as in Figure 2. The solid and broken lines correspond to the data in dilute and entangled regions, respectively.

Considering the J_e dependence on molecular weight and the concentration of added salt in dilute regions in Figure 2, we plotted J_eM^2/C_s vs C for PMVP-Cl in 0.5, 0.1, and 0.01 M NaCl solutions in Figure 3. From the figure, we have the following experimental relationship in dilute regions.

$$J_e \propto C^{-3}M^{-2}C_s \tag{6}$$

The slopes of solid lines in dilute regions in Figures 2 and 3 correspond to the concentration dependence of eq 6.

As shown by the broken lines in Figures 2 and 3, on the other hand, the deviation from eq 6 is observed in entangled regions, where the molecular weight dependence is not observed. In Figure 4, all the data in entangled regions are plotted in the double-logarithmic form of J_e vs C. From this figure, we have the following experimental relationship.

$$J_e \propto C^{-1.3} \tag{7}$$

The combination of eqs 6 and 7 indicates that for the higher molecular weight, or for the lower concentration of added salt, the crossover between the two regions occurs at the lower polymer concentration. Although the polymer concentration dependences of J_e are different from those of nonionic polymer solutions, the order of crossover concentrations is reasonable.

Discussion

Figure 5 shows double-logarithmic plots of J_{eR} vs MC for the data in Figure 2. As shown in the figure, J_{eR} is not

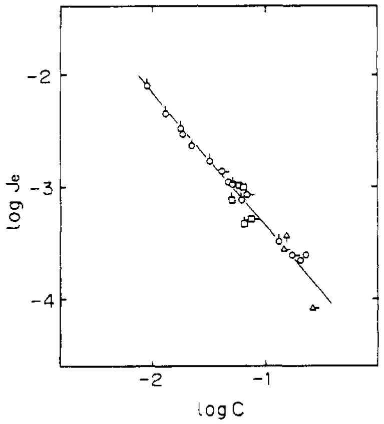

Figure 4. Double-logarithmic plots of J_e vs C in entangled regions. Symbols are the same as in Figure 2. The line denotes eq 7.

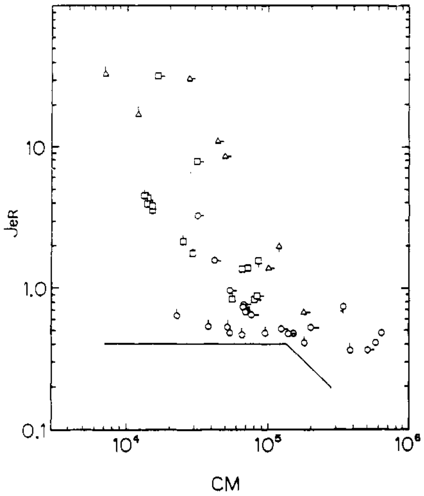

Figure 5. Double-logarithmic plots of J_{eR} vs CM. Symbols are the same as in Figure 2. The solid line denotes the data of polystyrene solutions.[2]

expressed as a univeral function of MC, and J_{eR} is not a constant in dilute regions, in contrast with that for nonionic polymer solutions. This result is due to the abnormal molecular weight and polymer concentration dependences shown in Figure 3. The molecular weight, added salt, and polymer concentration dependences as expressed in eq 6 may be qualitatively explained by considering that the stronger the electrostatic interactions, the higher the elasticity is. However, the quantitative description cannot be given at present. It should be noted that, even at high concentration of added salt, J_e of polyelectrolyte solutions do not approach that of nonionic polymer solutions at the present polymer concentrations, though the zero-shear viscosity can be described in the same manner as nonionic polymer solutions at high concentrations of added salt.[1]

In entangled regions, on the other hand, the experimental dependence on polymer concentration is lower than that of nonionic polymers. Therefore, we will discuss the effect of electrostatic interaction on J_e in entangled regions.

J_e or the inverse of the elastic modulus of polymer chains G in entangled regions is given by[11]

$$J_e \propto 1/G \propto n/(ck_BT) \qquad (8)$$

where c is the number of segments per unit volume, n is the number of segments between entanglement points, k_B is Boltzmann's constant, and T is the absolute temperature. Following the same procedure as in Part 1,[1] we can apply eq 8 to polyelectrolytes in entangled regions.

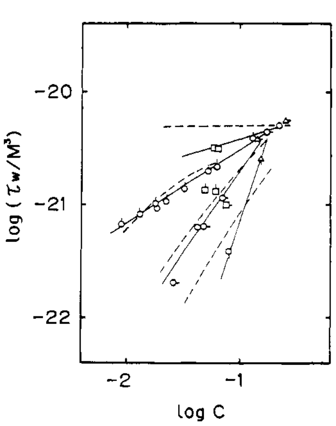

Figure 6. Double-logarithmic plots of τ_w/M^3 vs C at various concentrations of added salt in semidilute regions for η^0 and entangled regions for J_e. Symbols are the same as in Figure 2. The solid lines denote eq 20a–d from the top to the bottom. The broken lines denote eq 16 in 0, 0.01, 0.1, and 0.5 M NaCl solutions from the top to the bottom.

If we assume that the dimension of the chain between entanglement points a is proportional to the thermodynamic correlation length ξ in solutions, and, moreover, if we assume that the chain between entanglement points is expanded as a single chain by an expansion factor α, owing to the ideal Donnan effect as described previously, we have[1]

$$n \propto c\xi^3 \qquad (9)$$

$$a \propto \xi = bn^{1/2}\alpha \qquad (10)$$

$$\alpha^{-1} = K_1 n^{3/2}[(i^2c^2 + 4C_s{*}^2)^{1/2} - 2C_s{*}] \qquad (11)$$

where b is the segment length, K_1 is the constant defined in Part 1, and $C_s{*}$ is the concentration of added salt outside a polyion domain. Substituting eqs 9–11 into eq 8, we have

$$J_e \propto 1/[(i^2c^2 + 4C_s{*}^2)^{1/2} - 2C_s{*}]^{3/4}c^{3/4}k_BT \qquad (12)$$

If $C_s{*} \gg ic$, we have

$$J_e \propto 1/C^{9/4} \qquad (13)$$

This dependence corresponds to the prediction of the scaling law for nonionic polymers in good solvents. If $C_s{*} \ll ic$, on the other hand, we have

$$J_e \propto 1/C^{3/2} \qquad (14)$$

Since we can assume that $C_s{*} \ll ic$ in the entangled regions of the present samples, the polymer concentration dependence is predicted to be lower than that of nonionic polymers in entangled regions as given by eq 4. The experimental dependence (eq 7) agrees with this prediction, though it is slightly weaker than the calculated one (eq 14). The reason is not clear at present.

Finally, we will discuss the weight-averaged relaxation time τ_w given by eq 15 according to its definition.[12]

$$\tau_w = \eta^0 J_e \qquad (15)$$

It is to be noted that the longest relaxation time is the dominant term in τ_w for nonionic polymers.[13] Introducing eq 29 in Part 1[1] and eq 12 into eq 15, we have the following equation for τ_w in semidilute regions for η^0 and entangled regions for J_e

$$\tau_w \propto N^3[(i^2C^2 + 4C_s{*}^2)^{1/2} - 2C_s{*}]^{3/2}/c^{3/2} \qquad (16)$$

If the salt concentration is large enough, i.e., $ic \ll C_s{*}$, we have

$$\tau_w \propto N^3 c^{3/2} \tag{17}$$

This result corresponds to τ_w for nonionic polymers in good solvents according to the scaling law, though the experimental molecular weight and concentration dependences are slightly different as given by[14]

$$\tau_w \propto M^{3.4} C^{2.2} \tag{18}$$

In salt-free solutions, on the other hand, we have

$$\tau_w \propto N^3 \tag{19}$$

Thus the theory indicates that τ_w becomes independent of polymer concentration in salt-free solutions and the polymer concentration dependence increases with an increase in the concentration of added salt.

Using the experimental results for J_e given by eq 7 and for η^0 given by eq 5a–d in Part 1,[1] we have

$$\tau_w \propto M^3 C^{0.2} \qquad (C_s = 0\ \text{M}) \tag{20a}$$

$$\tau_w \propto M^3 C^{0.5} \qquad (C_s = 0.01\ \text{M}) \tag{20b}$$

$$\tau_w \propto M^3 C^{1.5} \qquad (C_s = 0.1\ \text{M}) \tag{20c}$$

$$\tau_w \propto M^3 C^{3.3} \qquad (C_s = 0.5\ \text{M}) \tag{20d}$$

The experimental results given by eq 20 reveal that the polymer concentration dependence of τ_w increases with an increase in the concentration of added salt and almost agrees with that for nonionic polymers in good solvents (eq 18) at high concentrations of added salt.[14]

Figure 6 shows double-logarithmic plots of τ_w/M^3 vs C in various NaCl solutions, together with eqs 16 and 20 denoted by the broken and the solid lines, respectively. Here, we assumed the effective charge $i = 0.2$ in eq 16 and shifted the calculated lines along the vertical axis to fit the data in the respective concentrations of added salt in the same manner as in Part 1.[1] From this figure we can conclude that the feature of the experimental polymer concentration dependence in the different concentration of added salt is well explained by the theory.

Introducing eq 6 and eq 5 in Part 1,[1] we have the following empirical equation for τ_w in semidilute regions for η^0 and dilute regions for J_e.

$$\tau_w \propto MC^{-1.2} \qquad (C_s = 0.01\ \text{M}) \tag{21b}$$

$$\tau_w \propto MC^{-0.2} \qquad (C_s = 0.1\ \text{M}) \tag{21c}$$

$$\tau_w \propto MC^{1.6} \qquad (C_s = 0.5\ \text{M}) \tag{21d}$$

These results are entirely different from that of nonionic polymers in good solvents given by $\tau_w \propto M^{4.4} C^{3.3}$, and we have no theory to explain eq 21.

In summary, we conclude that the linear viscoelastic properties of entangled polyelectrolyte solutions in the terminal region can be qualitatively explained by the reptation model taking into account the electrostatic interaction by Donnan equilibrium. In the above analysis, we assumed that the longest relaxation process is dominant in the terminal region as the first approximation. To understand the viscoelastic properties of polyelectrolyte solutions more in detail, further study is needed over a wide range of frequency.

Acknowledgment. We thank Rheometrics Far East Ltd. for the use of fluid spectrometers and the technical assistance with them. This work was supported by a Grant-in Aid for Scientific Research (No. 63430019) from the Ministry of Education, Science, and Culture of Japan.

References and Notes

(1) Part 1: Yamaguchi, M.; Wakutsu, M.; Takahashi, Y.; Noda, I., previous paper in this issue.
(2) Takahashi, Y.; Noda, I.; Nagasawa, M. *Macromolecules* **1985**, *18*, 2220.
(3) Konno, A.; Kaneko, M. *Makromol. Chem.* **1970**, *138*, 189.
(4) Sakai, M.; Noda, I.; Nagasawa, M. *J. Polym. Sci., Polym. Phys. Ed.* **1972**, *10*, 1972.
(5) Okamoto, H.; Nakajima, H.; Wada, Y. *J. Polym. Sci., Polym. Phys. Ed.* **1974**, *12*, 1035.
(6) Rosser, R. W.; Nemoto, N.; Schrag, J. L.; Ferry, J. D. *J. Polym. Sci., Polym. Phys. Ed.* **1978**, *16*, 1031.
(7) Suzuki, F.; Hori, K.; Kozuka, N.; Komoda, H.; Katsuro, K.; Takahashi, Y.; Noda, I.; Nagasawa, M. *Polym. J. (Tokyo)* **1986**, *18*, 911.
(8) Takahashi, Y.; Yamaguchi, M.; Hori, K.; Suzuki, F.; Noda, I. *Polym. J. (Tokyo)* **1989**, *21*, 815.
(9) Kriger, H. J. *Adv. Polym. Sci.* **1969**, *6*, 170.
(10) Tsvetkov, V. N. *Newer Methods of Polymer Characterization*; Ke, B., Eds.; Interscience: New York, 1964.
(11) Doi, M.; Edwards, S. F. *The Theory of Polymer Dynamics*; Clarendon Press: Oxford, 1986; Chapter 7.
(12) Graessley, W. W. *Adv. Polym. Sci.* **1974**, *16*, 1.
(13) Takahashi, Y.; Wakutsu, M.; Noda, I. *Macromolecules* **1990**, *23*, 242.
(14) Takahashi, Y.; Umeda, M.; Noda, I. *Macromolecules* **1988**, *21*, 2257.